ELSEVIER

Journal of Crystal Growth 236 (2002) 210–216

JOURNAL OF CRYSTAL GROWTH

www.elsevier.com/locate/jcrysgro

Crystal growth and characterization of new high Curie temperature $(1-x)BiScO_3$–$xPbTiO_3$ single crystals

Shujun Zhang*, Laurent Lebrun, Sorah Rhee, Richard E. Eitel, Clive A. Randall, Thomas R. Shrout

Materials Research Laboratory, Pennsylvania State University, University Park, PA, 16802-4801, USA

Received 7 November 2001; accepted 13 November 2001
Communicated by Dr. M. Schieber

Abstract

Novel perovskite ferroelectric $(1-x)BiScO_3$–$xPbTiO_3$ single crystals with tetragonal phase were successfully grown by a conventional high-temperature solution method using a Pb_3O_4 and Bi_2O_3 flux. The typical crystal size was 2–15 mm with rectangular shape and green/blue color. The dielectric constant (K) at room temperature was determined to be 400–550, decreasing to about 300 after the poling process. The Curie temperature of $0.43BiScO_3$–$0.66PbTiO_3$ single crystals was found to be about 460°C, similar to the polycrystalline data. The remanent polarization (P_r) was 28 μC/cm^2 with a coercive field (E_c) of 34 kV/cm. The piezoelectric coefficient d_{33} was about 200 pC/N for $\langle 0\,0\,1\rangle$-oriented tetragonal crystals. The longitudinal electromechanical coupling coefficient k_{33} was ~73% with a lateral mode coupling coefficient k_{31} of ~−35.8% and a thickness mode coupling k_t of 60–64%.

PACS: 77.84.−s; 77.84.Dy; 81.10.Dn; 77.65.Bn; 77.80.Bh

Keywords: A2. Single crystal growth; B1. Perovskite; B2. Ferroelectric materials; B2. Piezoelectric materials

1. Introduction

Piezoelectric materials have been the subject of investigations since the development of perovskite ferroelectrics $BaTiO_3$ and $Pb(Zr_{1-x}Ti_x)O_3$ (PZT) in the 1950s [1]. They are widely used in underwater sonar, modern medical ultrasound imaging and other high performance actuator and transducers. For high-performance piezoelectrics, their implementation may be limited either by the corresponding low Curie temperature or by the low piezoelectric activity associated with higher T_c ferroelectrics. In the past 10 years, single crystals of the solid solution of $Pb(Zn_{1/3}Nb_{2/3})O_3$–$PbTiO_3$ (PZNT) [2–5] and $Pb(Mg_{1/3}Nb_{2/3})O_3$–$PbTiO_3$ (PMNT) [6,7] have been studied as another method to improve device performance through enhanced piezoelectric activity and electromechanical coupling. Longitudinal electromechanical coupling as high as 90% and piezoelectric coefficients d_{33} ~2500 pC/N have been reported for PZNT [4] and PMNT [7] single crystals. The

*Corresponding author. Tel.: +1-814-863-2639.
E-mail address: sozl@psu.edu (S. Zhang).

0022-0248/02/$ - see front matter
PII: S0022-0248(01)02093-0

properties of these crystals are critically dependent upon the compositions as with PZT, lying near their morphotropic phase boundary (MPB). Their Curie temperature (T_c) at 150–180°C, is much lower than that of the conventional PZT ceramic, being limited further by the rhombohedral to tetragonal phase transition temperature, T_r of ~90°C. Hence, new crystals with higher Curie temperature are desired. Yasuda et al. reported single crystals in the system $Pb(In_{1/2}Nb_{1/2})O_3$–$PbTiO_3$ (PINT) whose Curie temperature was reported to be about 260°C with a piezoelectric coefficient d_{33} of 700 pC/N [8,9]. Furthermore, perovskite single crystals in the $(1-x)Pb(Yb_{1/2}Nb_{1/2})O_3$–$xPbTiO_3$ (PYN–PT) system have been studied [10]. It was found that near the MPB, the Curie temperature was around 350°C, the piezoelectric coefficient was up to 2500 pC/N [11].

Recently, a novel MPB system with significantly higher Curie temperature while maintaining large piezoelectric coefficients, $(1-x)BiScO_3$–$xPbTiO_3$ (BSPT) was reported in polycrystalline ceramics [12]. In this work, attempts to grow BSPT single crystals were explored and the properties of single crystals reported.

2. Crystal growth

Single-crystal BSPT with a composition $x = 0.66$, reported near the MPB, was grown using a self-flux method. High-purity powders Pb_3O_4 (Alfa Aesar), Bi_2O_3 (Alfa Aesar), Sc_2O_3 (PIDC) and TiO_2 (Alfa Aesar) were used as starting materials. Pb_3O_4 and Bi_2O_3 with ratios according to the PbO–Bi_2O_3 phase diagram were selected as the flux owing to their low melting temperature and chemical compatibility with the stability compositions. Sintered BSPT polycrystalline material and various ratios of flux were loaded into platinum (Pt) crucibles, which was sealed by a 0.03 mm-thick Pt foil to minimize the evaporation of the flux. The Pt crucibles were then put into an alumina crucible sealed with alumina lid and alumina cement. The growth was carried out in a muffled resistance furnace. The materials were heated to 1200°C and soaked for 7 h, followed by slow cooling (0.1–5°C/h) to 900°C. The crucible was then furnace-cooled to room temperature.

Fig. 1. The photo of BSPT single crystals with rectangular shape.

As-grown single crystals of BSPT are shown in Fig. 1. The crystals obtained were green/blue in color and transparent with 2–15 mm in size. The typical single crystals are rectangular in shape with pseudocubic (0 0 1) faces in habit. The main defects in the BSPT single crystals are flux inclusions and (0 0 1) cleavage planes. The X-ray powder diffraction (XRD) performed on ground single crystal is shown in Fig. 2a indicating that the crystals are tetragonal. Fig. 2b is the X-ray diffraction of the emerged faces on the crystal, which revealed that the habitual faces of the obtained crystal are {0 0 1}. The c/a ratio of BSPT single crystal calculated from Fig. 2b is 1.03, which is larger than that of PZNT (c/a ratio for PZNT crystal is 1.02 [4]). A c/a ratio of 1.03 corresponded to a BSPT66 as reported by Eitel et al. [12] for polycrystalline materials just on the tetragonal side of MPB. The density of BSPT single crystal was measured to be 7.5 g/cm^3 which is very close to the polycrystalline materials [12].

3. Dielectric and piezoelectric properties of BSPT single crystal

The samples for dielectric and piezoelectric measurements were oriented along their

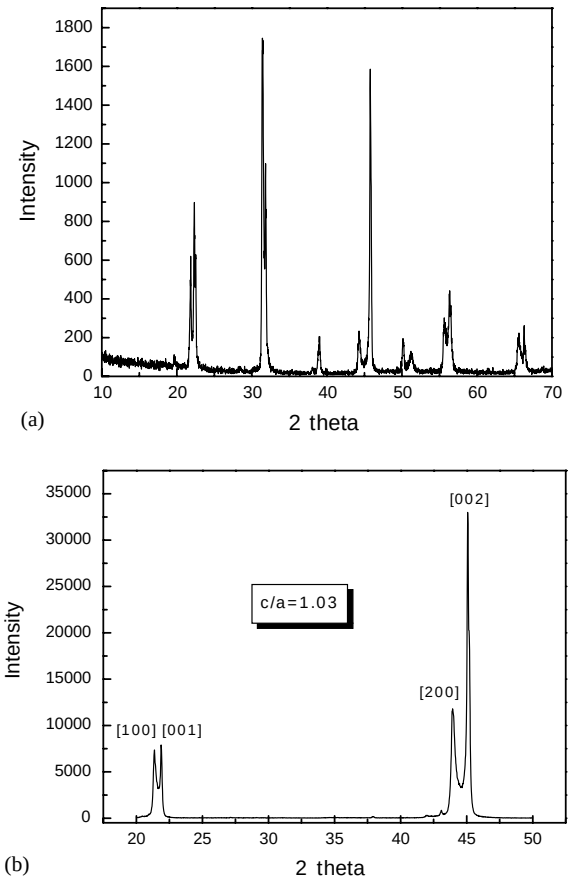

Fig. 2. XRD of BSPT single crystals with tetragonal phase. (a) BSPT powder (b) habitual growth face indicate {0 0 1}.

crystallographic direction ⟨0 0 1⟩ using a real-time Laue orientation system (Multiwire Laboratories, Ltd). The sample size was about 0.5–1.0 mm in thickness and 8–25 mm^2 in area. Dielectric properties with temperature were determined using a multi-frequency LCR meter (HP 4284A) from room temperature to 500°C. Polarization and strain hysteresis were measured using a modified Sawyer–Tower circuit driven by a lock-in amplifier (Stanford Research Systems, Model SR830). High electric fields were obtained using a Trek 609C-6 high-voltage DC amplifier. An impedance analyzer (HP4194A) was used to measure the resonance frequency and the anti-resonance frequency. The samples for measuring electromechanical coupling coefficients were poled at 120°C and 50 kV/cm electric field.

4. Results and discussion

4.1. Dielectric properties

The room temperature dielectric constant was found to vary between 400 and 550, with dielectric loss tangents about 0.5%. After high-temperature poling, the dielectric constant decreased to about 300, as reported for other tetragonal ferroelectrics such as $PbTiO_3$, etc. Fig. 3 presents the dielectric constant and loss temperature dependence of the BSPT single crystals at 10 and 100 kHz frequencies. The dielectric maximum occurred at about 460°C, indicating the ferroelectric to paraelectric cubic phase transition temperature (Curie temperature). It is important to note that this T_c is much higher than PZNT and PMNT perovskite crystals (about 150–180°C) [7,13]. Compared with the Curie temperature of the BSPT polycrystalline materials [12], the PT content in the BSPT single crystals is about 66%, which is in the tetragonal region, as confirmed by the c/a ratio. The dielectric loss tangent also showed a maximum in the vicinity of Curie temperature and increases rapidly with heating, this increase is associated with a conductive loss.

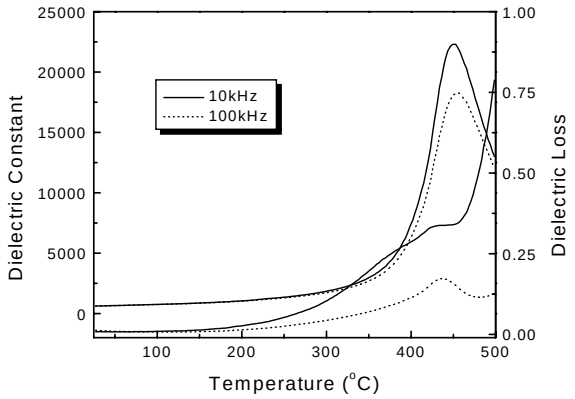

Fig. 3. Dielectric constant and dielectric loss of BSPT66 single crystal as the function of temperature.

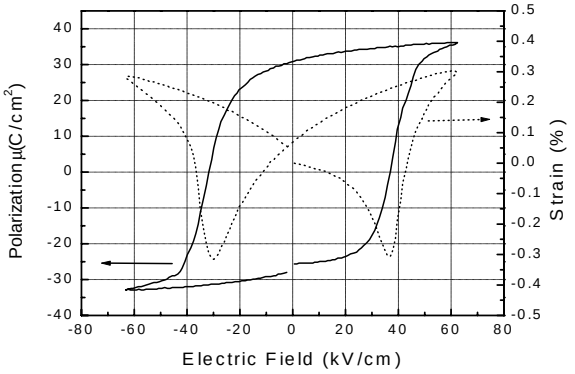

Fig. 4. Polarization and strain vs. electric field (bipolar) curve for ⟨0 0 1⟩-oriented BSPT66 tetragonal single crystal.

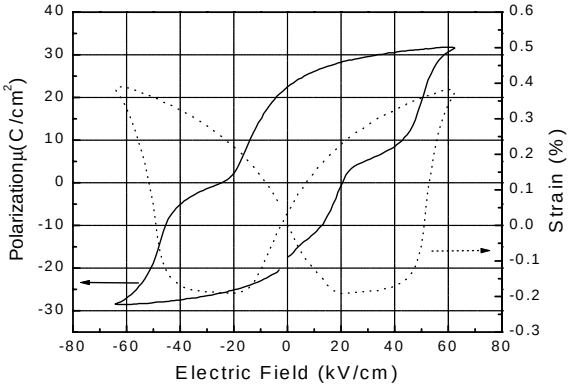

Fig. 5. Constrained *P–E* hysteresis loop and strain-field loop for BSPT single crystal caused by the domain wall pinning with oxygen vacancies.

4.2. Piezoelectric properties

Fig. 4 shows a typical polarization-electric field hysteresis loop of a BSPT single crystal measured at room temperature under an electric field of 60 kV/cm and a frequency of 0.5 Hz. A remanent polarization of Pr of 28 μC/cm^2 and coercive field E_c of 34 kV/cm were obtained from the loop. The coercive field found is significantly higher than that of PZNT tetragonal single crystal being of the order of 3–5 kV/cm. Strain-field data, for the same measured conditions, are also given in Fig. 4, which follow the classical bipolar ferroelectric switching behavior, displaying a symmetric butterfly loop. A constrained pinched *P–E* hysteresis behavior and strain behavior were obtained for another sample from the same growth run, shown in Fig. 5, similar to that for 'hard' piezoelectric ceramics reported previously [14]. A possible reason for the constrained loop is a defect dipole created by an association between an acceptor charge and a compensate oxygen vacancy, pinning the walls, and preventing nucleation and growth of domains in the direction favored by an applied electric field.

Fig. 6 presents the strain-field curve measured at 60 kV/cm for a ⟨0 0 1⟩-oriented sample after poling at 120°C and 50 kV/cm field for 15 min. As shown, the strain-*E* field hysteresis is very low with a calculated d_{33} of ~200 pC/N, similar to the value obtained using a Berlincourt d_{33} meter.

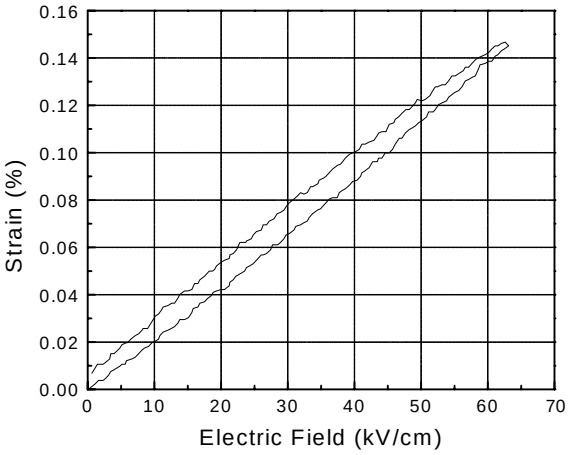

Fig. 6. Strain vs. electric field (unipolar) for ⟨0 0 1⟩-oriented BSPT66 tetragonal single crystal after the poling at 120°C and 50 kV/cm.

4.3. Electromechanical properties

The resonance and antiresonance frequency characteristics of impedance and phase for the ⟨0 0 1⟩-oriented BSPT66 single crystals for a longitudinal mode measured at room temperature, 150°C and 250°C are shown in Fig. 7a. The longitudinal electromechanical coupling coefficient k_{33} is ~73% at room temperature increasing to 80% at 250°C, as presented in Fig. 7b. The

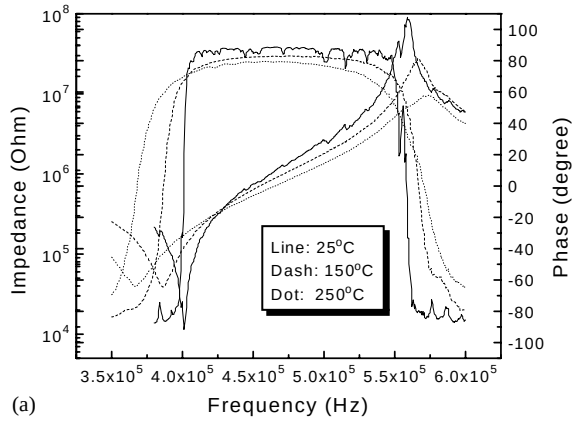

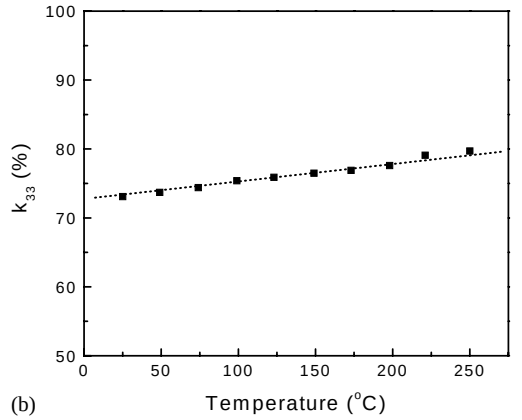

Fig. 7. (a) Resonance and antiresonance frequency characteristics of impedance and phase for the ⟨0 0 1⟩-oriented BSPT66 single crystal in the k_{33} mode with different temperatures. (b) Longitudinal electromechanical coupling coefficient k_{33} with different temperatures.

transverse electromechanical coupling coefficient, k_{31} was determined to be $\sim -35.8\%$ and the thickness electromechanical quality factor k_t was about 60–64%. Mechanical coupling coefficient Q was found to be 20–200 of the order of a few hundreds. The detailed properties of BSPT66 tetragonal single crystal are listed in. As reported in Table 1, a d_{33} of ~ 180 pC/N was calculated from k_{33}, which is similar to the direct measurement value. Again similar to other tetragonal systems, the large anisotropic of large d_{33}–d_{31} leads to an expectedly high d_h value larger than 90 pC/N. Also, listed in the table are the elastic compliances S_{11}^E, S_{33}^D and S_{33}^E calculated from the resonance and antiresonance frequencies.

4.4. Temperature dependence of AC conductivity

The conductivity σ was calculated by assuming that the sample could be modeled as a leaky capacitor, i.e. capacitor (C) in parallel with a resistor (R). In this case, the dielectric loss:

$$\tan\delta = 1/2\pi fRC, \tag{1}$$

where f is the frequency.

$$\sigma = l/RS, \tag{2}$$

where S is the area and l is the thickness of the sample.

Using the automated equipment previously described, $\tan\delta$ and dielectric constant are recorded vs. temperature, which are shown in Fig. 3.

Finally,

$$\sigma = 2\pi f \varepsilon_0 \varepsilon_r \tan\delta. \tag{3}$$

Fig. 8 shows the evolution of $\ln(\sigma)$ vs. $1/T$. It could be modeled by the Arrhenius law:

$$\sigma = A\exp\left(\frac{-E_a}{kT}\right), \tag{4}$$

$$\ln\sigma = \ln A - \frac{E_a}{kT}, \tag{5}$$

where the A is the pre-exponential term, k is the Boltzmann constant, E_a is the conduction activation energy. E_a calculated from the experimental data and equal to 0.93 eV in the high temperature range, which is close to the previous values reported for vacancies conductivity mechanism 1 eV for oxygen vacancy [15,16].

Attempts to anneal the crystals in oxygen atmosphere were unsuccessful. We therefore anticipate the oxygen vacancy concentration is ionically compensated by an acceptor charge. One possible mechanism for this source or charge could be the relative difference in volatility between Bi_2O_3 and PbO, with a greater loss of Bi_2O_3 from the flux during the crystal growth. There could be an excess of Pb^{2+} at the Bi^{3+} sites. That is ionically compensated by oxygen vacancies: $[Pb_{Bi}^{2+}] = 2[V_{\ddot{O}}]$.

Table 1
The electrical properties of the BSPT66 tetragonal single crystals

BSPT tetragonal single crystal								
Orientation	Density	T_c	$\tan\delta$	P_r	E_c	k_{33}	k_{31}	k_t
⟨0 0 1⟩	7.5 g/cm^3	460°C	0.5%	28 μC/cm^2	34 kV/cm	73%	−35.8%	60–64%
d_{33} (measured) (pC/N)	d_{33} (calculated) (pC/N)	d_{31} (pC/N)	d_h (pC/N)	Q_m	Q_t	S_{11}^E (m^2/N)	S_{33}^D (m^2/N)	S_{33}^E (m^2/N)
200	180	−44	>90	200	20–100	5.39×10^{-12}	10.43×10^{-12}	22.32×10^{-12}

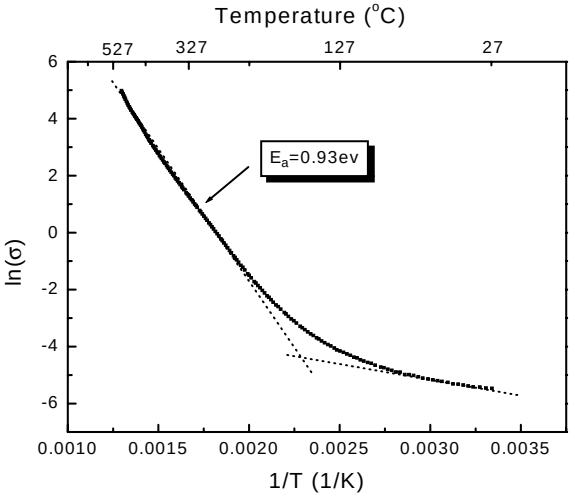

Fig. 8. $\ln(\sigma)$ vs. $1/T$ curve for BSPT66 single crystal.

In the low-temperature range, the E_a is only 0.1 eV, which may be corresponded to an electronic conductivity, the major electronic carrier species. This will be discussed in another paper.

5. Conclusions

In summary, perovskite BSPT single crystals ($x = 0.66$) with tetragonal phase near the MPB composition were grown using a high-temperature flux method. Typical crystals obtained were rectangular being 2–15 mm in size and green/blue in color. The room temperature dielectric constant was ~300 after high-temperature poling. The Curie temperature for BSPT66 single crystals was 460°C. A coercive field of about 34 kV/cm for ⟨0 0 1⟩-oriented BSPT66 tetragonal crystal, which is much higher than other tetragonal crystals, such as PZNT and PMNT. The d_{33} of the tetragonal BSPT66 crystal was found to be about 200 pC/N with large longitudinal electromechanical coupling coefficient, k_{33} about 73%, increasing to 80% at 250°C. The thickness electromechanical coupling coefficient k_t was about 60–64%. Combined with the low dielectric constant, tetragonal BSPT may be a good candidate for the single-element transducer in ultrasound application. The rhombohedral BSPT crystal should exhibit high E-induced strain and high Curie temperature owing to a large c/a ratio of 1.03, which makes it a promising material for the next generation high-temperature and high-performance actuator and transducer applications.

Acknowledgements

This research was supported by the ONR and DARPA. The author would like to thank Ru Xia for the crystal processing.

References

[1] B. Jaffe, J. Res. Natl. Bur. Stand. 55 (1955) 239.
[2] S.-E. Park, T.R. Shrout, J. Mater. Res. Innov. 1 (1997) 20.
[3] S.-E. Park, T.R. Shrout, Jpn. J. Appl. Phys. 36 (1997) 1154.
[4] S.-E. Park, T.R. Shrout, J. Appl. Phys. 82 (1997) 1804.
[5] S. Shimanuki, S. Saito, Y. Yamashita, Jpn. J. Appl. Phys. 37 (1998) 3382.
[6] M. Dong, Z.-G. Ye, J. Crystal Growth 209 (2000) 81.
[7] H.S. Luo, G.S. Xu, Z.W. Yin, Jpn. J. Appl. Phys. 39 (2000) 5581.
[8] N. Yasuda, H. Ohwa, M. Kume, Y. Yamashita, J. Crystal Growth 229 (2001) 299.
[9] N. Yasuda, H. Ohwa, Y. Yamashita, Jpn. J. Appl. Phys. 39 (2000) 5586.

[10] S.J. Zhang, P.W. Rehrig, C.A. Randall, T.R. Shrout, J. Crystal Growth 234 (2002) 415.
[11] S.J. Zhang, C.A. Randall, T.R. Shrout, Jpn. J. Appl. Phys. 41 (2002) 2A.
[12] R. Eitel, C.A. Randall, T.R. Shrout, P. Rehrig, W. Hackenberger, S.-E. Park, Jpn. J. Appl. Phys. 40 (2001) 5999.
[13] J. Kuwata, K. Uchino, S. Nomura, Ferroelectrics 37 (1981) 579.
[14] X. Dai, Z. Xu, D. Viehland, J. Am. Ceram. Soc. 78 (1995) 2815.
[15] M.V. Raymond, D.M. Smyth, J. Phys. Chem. Solids. 57 (1996) 1507.
[16] D.M. Smyth, Ferroelectrics 151 (1994) 115.